Chapter 2
Adsorption Calorimetry on Well-Defined Surfaces

Ole Lytken, Hans-Jörg Drescher, Rickmer Kose, and J. Michael Gottfried

Abstract The focus of this chapter is single-crystal adsorption calorimetry, which is used for the direct measurement of adsorption energies on well-defined surfaces, both single- and poly-crystalline. The method was pioneered in the 1990s mainly by D.A. King and C.T. Campbell and is based on earlier work by S. Černy. Especially in recent years, the technique has seen increasing proliferation and development. In contrast to desorption-based methods, such as temperature-programmed desorption and isosteric measurements, calorimetry is also well suited for irreversible reactions. The systems studied range from simple adsorption of small molecules, such as CO and NO, to surface reconstructions, reaction intermediates, hydroxyl group formation, metal adsorption and diffusion into polymers, particle-size dependent adsorption energies on model catalysts and even electrochemical reactions on electrode surfaces in the liquid phase.

2.1 Introduction

Adsorption processes are of fundamental importance for heterogeneous catalysis, sensor technology, and electrochemical processes, but also for the production of thin films, for example in semiconductor technology. One of the most important

O. Lytken (✉)
Lehrstuhl für Physikalische Chemie II, Universität Erlangen-Nürnberg, Egerlandstr. 3, 91058 Erlangen, Germany
e-mail: ole.lytken@chemie.uni-erlangen.de

R. Kose
Sentys Inc, 182 Howard St #750, San Francisco, CA 94105, USA
e-mail: rkose@sentys.com

H.-J. Drescher · J.M. Gottfried (✉)
Fachbereich Chemie, Philipps-Universität Marburg, Hans-Meerwein-Straße 6, 35032 Marburg, Germany
e-mail: michael.gottfried@chemie.uni-marburg.de

H.-J. Drescher
e-mail: hans-joerg.drescher@chemie.uni-marburg.de

parameters in this respect is the adsorption energy as a direct measure for the strength of the interaction between the adsorbate and the surface [1]. For example, the catalytic activation of a molecule requires a sufficiently strong interaction of the intermediate with the surface of the catalyst; the same is true for the bonding of a molecule to a sensor and for electrochemical and electrocatalytic processes. However, if the adsorptive bond is too strong, the adsorption will lead to a poisoning of the catalyst (principle of Sabatier) [2]. The precise knowledge of experimental adsorption energies is also important for the improvement of theoretical methods, especially as focus shifts toward larger molecules and more complex systems. Single-crystal adsorption calorimetry measures the heat of reaction as an adsorbate adsorbs on a surface and is a very versatile tool, able to provide information not available with any other technique. Although the technique started out with a narrow focus on single-crystal studies, it has now become a more general technique for planar, low surface area systems.

2.2 Theory Background

2.2.1 Approaches for the Measurement of Adsorption Energies

Adsorption energies can be determined by thermodynamic and, indirectly, kinetic methods. Temperature-programmed desorption (TPD, also known as thermal desorption spectroscopy) [3, 4] belongs to the kinetic methods. Here, the desorption rate constant r is measured as a function of temperature T, and the desorption activation energy E_a is then determined using the simple rate equation (also Polanyi-Wigner equation):

$$r = \nu \exp\left(-\frac{E_a}{RT}\right)\Theta^n \tag{2.1}$$

where Θ is the coverage and n the desorption order. In the case of non-activated adsorption, the activation energy for desorption approximates the negative adsorption energy. Another classical approach is based on equilibrium thermodynamics and considers the change of the equilibrium pressure p with temperature at constant coverage. These quantities are related by the Clausius-Clapeyron equation to the heat of adsorption at constant coverage (isosteric heat) [1]:

$$q_{st} = -R\left(\frac{\partial \ln p}{\partial(1/T)}\right)_{\Theta} \tag{2.2}$$

The major limitation of both methods is that they can be applied only in cases of fully reversible adsorption, i.e., when the molecules desorb much faster than they decompose; a classical example is carbon monoxide desorbing from a Pt(111) surface (Fig. 2.1a). Many molecules, especially large organic or biomolecules, however, dissociate on the surface and only their fragments desorb. An example is benzene on Pt(111) (Fig. 2.1b), which adsorbs intact at room temperature and below, but decomposes at elevated temperatures forming carbon (in graphene-like structures [5])

Fig. 2.1 Reversible and irreversible adsorption. (**a**) Reversible: CO on Pt(111). CO desorbs intact and the molar adsorption energy ΔU_{ads} can be estimated from the desorption activation energy E_{des}. (**b**) Irreversible: Benzene on Pt(111). Benzene adsorbs at 300 K as an intact molecule, but dissociates above 500 K forming hydrogen and carbon. In this case, calorimetry is needed to determine ΔU_{ads} (images courtesy E.K. Vestergaard)
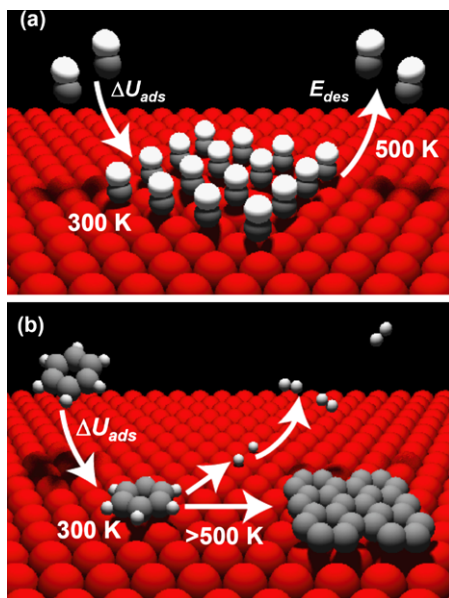
and hydrogen, which desorbs. In this case, neither TPD nor methods based on the Clausius-Clapeyron equation (2.2) can be used. For such systems, the adsorption energy can only be determined by direct calorimetric measurement, i.e., by measuring the temperature increase due to the heat of adsorption.

2.2.2 Thermodynamics

The following considerations focus on the thermodynamic understanding of the ultrahigh vacuum-based calorimeters, especially the Campbell calorimeter (see Sect. 2.3.3). A typical experiment consists of a pulsed molecular beam striking a single-crystal sample. As each pulse strikes the sample, heat is deposited and measured as a temperature change in the sample. Simultaneously for each pulse the sticking probability (fraction of the molecules in each pulse adsorbing on the sample) is measured, and with knowledge of the amount of molecules per pulse, the number of molecules that adsorbed on the sample may be calculated. Because of the approximately isochore conditions in the ultrahigh vacuum apparatus, the heat measured (q_{cal}) is equivalent to the change of the internal energy of the sample (Δu_p). (Note that we use lowercase letters for extensive quantities and uppercase letters for intensive quantities.) Δu_p contains two contributions: one from molecules that adsorbed on the sample ($\Delta u_\downarrow$), and another from molecules that were reflected, but exchanged energy with the sample ($\Delta u_{\downarrow\uparrow}$):

$$q_{cal} = \Delta u_p = \Delta u_\downarrow + \Delta u_{\downarrow\uparrow} \tag{2.3}$$

$\Delta u_\downarrow$ can be expressed as the sum of three terms: (i) the actual adsorption energy Δu_{ads}, i.e., the change of the internal energy of the system gas/surface during adsorption of a gas with the sample temperature T_p, (ii) a term $\frac{1}{2}RT_{ms}$ for the energy difference between a gas *flux* and a gas *volume* at the temperature of the molecular beam source, T_{ms} [6], (iii) a contribution due to the gas temperature T_{ms} being different than the sample temperature T_p:

$$\Delta u_\downarrow = -\Delta u_{ads} + n_{ads}\left(\frac{1}{2}RT_{ms} - \int_{T_{ms}}^{T_p} C_v\, dT\right) \tag{2.4}$$

where n_{ads} is the adsorbed amount of gas (in mol) and C_v is the molar isochore heat capacity of the gas. Note that Δu_{ads} contributes to (2.4) with a negative sign, because the system gas/surface releases heat ($\Delta u_{ads} < 0$), but the sample considered here gains this amount of heat ($\Delta u_\downarrow > 0$).

The integral term in (2.4) is relevant when the temperature of the molecular beam source is different from the sample temperature and, as mentioned above, also reflected molecules can contribute to q_{cal} by exchanging energy with the sample (term $\Delta u_{\downarrow\uparrow}$ in (2.3)). Assuming that all reflected molecules leave the surface with the sample temperature T_p, i.e., that complete thermalization occurs, the following equation is obtained:

$$\Delta u_{\downarrow\uparrow} = -n_{refl}\int_{T_{ms}}^{T_p}\left(C_v + \frac{1}{2}R\right)dT \tag{2.5}$$

where n_{refl} is the reflected amount of gas. The additional term $\frac{1}{2}R$ takes into account that a flux of molecules is warmer than the corresponding volume of gas. If the volume of gas is in thermal equilibrium this corresponds to $\frac{1}{2}R$ [6].

The *adsorption enthalpy*, Δh_{ads}, at T_p equals the adsorption energy Δu_{ads} plus the volume work, which would result, under isobaric conditions, from the compressions of the gas phase (assumed to be ideal) to the negligibly small volume of the adsorbed phase:

$$\Delta h_{ads} = \Delta u_{ads} - n_{ads}RT_p \tag{2.6}$$

This quantity allows for comparison with tabulated thermodynamic standard quantities (after conversion to standard temperature, if necessary).
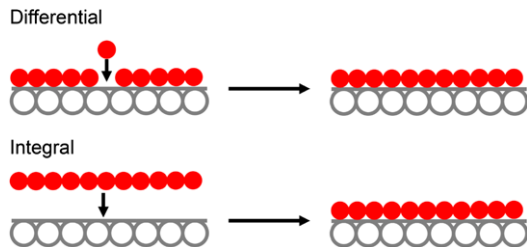
The *molar heat of adsorption* is normally defined as the negative molar adsorption enthalpy, $-\Delta H_{ads}$, and thus always positive. Combining (2.3)–(2.6) results in the following relation between $-\Delta H_{ads}$ and the measured heat q_{cal}:

$$-\Delta H_{ads} = \frac{-\Delta h_{ads}}{n_{ads}} = \frac{1}{n_{ads}}(q_{cal} - K_{ads} - K_{refl}) \tag{2.7}$$

with the correction terms

$$K_{ads} = n_{ads}\left[-\int_{T_{ms}}^{T_p} C_v\, dT + \frac{1}{2}RT_{ms} - RT_p\right] \tag{2.8}$$

$$K_{refl} = n_{refl}\left[-\int_{T_{ms}}^{T_p}\left(C_v + \frac{1}{2}R\right)dT\right] \tag{2.9}$$

Fig. 2.2 Differential (*top*) and integral (*bottom*) heats of adsorption near saturation coverage. In the case of the differential heat of adsorption, differentially small changes of coverage are considered, while the integral heat of adsorption considers finite changes starting from $\Theta = 0$. Calorimetric experiments typically measure the differential heat of adsorption, whereas theoretical calculations typically calculate the integral heat of adsorption

$-\Delta H_{ads}$ is a differential heat of adsorption. Integration of $-\Delta H_{ads}$ over the coverage Θ yields the respective integral heat of adsorption $-\Delta H_{ads,int}$ (see Fig. 2.2):

$$-\Delta H_{ads,int} = -1/\Theta \int_0^{\Theta} \Delta H_{ads} \, d\Theta' \tag{2.10}$$

Integral and differential heats and energies of adsorption play an important role for comparisons with results from ab-initio calculations. For such comparison, it can be useful to take the changes in the internal and external degrees of freedom (DOF) of the adsorbing molecules into account. In the simplest case, a mono-atomic gas (three translational DOF), the enthalpy of the gas is given by (with $T = 0$ as the point of reference):

$$H_{gas} = U_{gas} + pV_{gas} = \frac{3}{2}RT + RT \tag{2.11}$$

For estimating the enthalpy of the adsorbed phase, H_{ads}, one needs to distinguish between mobile and localized adsorption. In the case of mobile adsorption, the molecule has two lateral translational DOF ($F_{trans} = 2$) and one vibrational DOF ($F_{vib} = 1$) perpendicular to the surface. For full excitation of all DOF, this results in (again with $T = 0$ as reference point):

$$H_{ads} = U_{ads} = -|E_0| + 2RT \tag{2.12}$$

where $|E_0|$ is the adsorbate-substrate bond energy. Thus, the following relation holds for the heat of adsorption:

$$\Delta H_{ads} = H_{gas} - H_{ads} = -|E_0| + \frac{1}{2}RT \tag{2.13}$$

In contrast, for localized adsorption ($F_{trans} = 0$, $F_{vib} = 3$), one obtains in the case of full excitation of all DOF:

$$\Delta H_{ads} = H_{gas} - H_{ads} = -|E_0| - \frac{1}{2}RT \tag{2.14}$$

$|E_0|$ can now be compared to calculated adsorbate-substrate bond energies or (in the case of non-activated adsorption) to desorption activation energies E_{des}.

The situation can become very complex, especially in the case of large molecules, because in principle the adsorption-induced changes in the excitation of internal degrees of freedom must be taken into account. This holds in particular for chemisorption, which influences the chemical bonds in the molecule, and thus, via the partition functions, the contribution of the vibrations to the total energy. However, these contributions are in the order of RT ($\sim$2.5 kJ/mol at 300 K) and thus much smaller than typical adsorption energies for large molecules.

2.3 Experimental Setup and Method

2.3.1 History

Adsorption calorimetry on thin metal wires, which serve as both substrates and resistance thermometers, were already performed in the 1930s by J.K. Roberts with the focus on a quantitative understanding of chemisorption and adsorbate-adsorbate interactions. For example, the adsorption of H_2, N_2 and O_2 on tungsten was investigated with this approach [7–9]. P. Kisliuk later improved this method by using metal ribbons instead of wires to achieve a higher surface-to-volume ratio [10]. Until the 1970s, this approach was pursued by various groups [11]. However, it became evident that the polycrystalline samples with their wide spectrum of different adsorption sites lead to problems with the reproducibility of results, especially as the wire and ribbon samples were also structurally and chemically insufficiently defined.

Around 1940, O. Beeck [12, 13] introduced the thin film calorimeter, in which vapor-deposited metal films are used. This technique was later improved and extensively used by G. Wedler [14–17] and by a number of other groups. The Wedler calorimeter (Fig. 2.3) contains a thin-walled round glass bulb (1) with a metal filament (4) inside, from which the metal is vapor-deposited onto the inner wall of the bulb as a thin closed film. Around the outside of the bulb, a thin metal wire is wound in a induction-free loop arrangement as a resistance thermometer. The gas is introduced into the evacuated bulb in small pulses, while the adsorption-induced temperature change of the bulb is measured. For thermal insulation, the glass bulb is located inside an evacuated glass cylinder (6), which is immersed in a thermostat. The heat capacity of this calorimeter is in the order of 1 J/K, and temperature changes as low as 1 µK can be detected [11, 16, 17]. With an active sample surface of 75 cm^2, absolute sensitivities in the range of 10 nJ/cm^2 are reached. For calibration of the Wedler calorimeter, the resistance thermometer is used as a resistance heater to deposit a precisely known amount of heat. This calorimeter type was used for adsorption studies of various small molecules on transition metal films [11]. A disadvantage of the technique is again the polycrystalline nature of the metal films, the dependence of the film morphology on the deposition parameters and the very limited possibilities for a structural and chemical characterization of the surface.
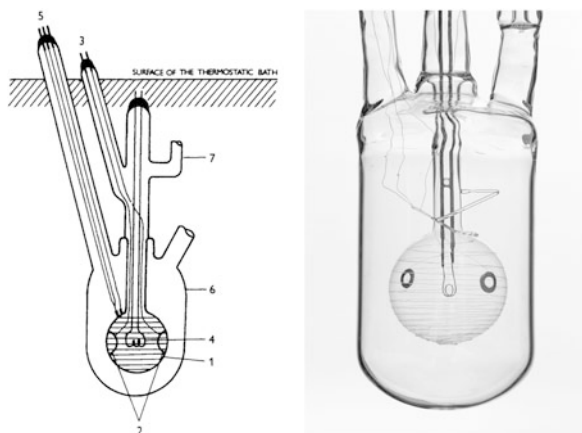
Fig. 2.3 Spherical adsorption calorimeter after Wedler [16, 17]. (*1*) Thin-walled glass bulb (∅ 5 cm, wall thickness 0.1 mm) with resistance thermometer on the outside (tungsten, length 2 m, ∅ 10 μm). (*2*) Platinum contact foils for measuring the resistance of the film and the related electrical feedthroughs (*3*). (*4*) Evaporant (metal wire). (*5*) Electrical feedthroughs for the resistance thermometer. (*6*) Evacuated glass bulb for thermal insulation (*left figure* reproduced from Ref. [11] with permission from Elsevier B.V., © 1996)

The adsorption calorimeter by S. Černý et al. [18] relies on a principle similar to that of the single-crystal calorimeters by King and Campbell, which will be described in the next section, and was developed independently around the same time. The Černý calorimeter uses a pyroelectric detector (LiTaO$_3$), onto which the sample is vapor-deposited as a thin polycrystalline metal film. The molecules are dosed with a pulsed supersonic molecular beam. For calibration, a laser beam is used, which takes the same path as the molecular beam.

Finally, we mention the micromechanical calorimeter [19–22], which uses the temperature-induced bending of a bimetallic cantilever for the detection of heats of adsorption and reaction. A typical Si/Al cantilever has a length of ∼400 μm, a width of 35 μm, and a thickness of ∼1.5 μm. The bending is measured similarly as in an Atomic Force Microscope. The calorimeter reaches an absolute sensitivity limit of ∼10^{-12} J, which corresponds to ∼10 nJ/cm^2. Thus, the sensitivity per area is similar to that of the Wedler calorimeter, and both are limited to polycrystalline substrates.

For a more detailed description of the history of adsorption calorimetry, we refer to Ref. [11].

2.3.2 Single-Crystal Adsorption Calorimeter by D.A. King

The major challenge of adsorption calorimetry is to ensure that the heat released upon adsorption causes a measurable change in temperature, which requires the

heat capacity to be low in relation to the heat of adsorption, which is proportional to the surface area. This condition is typically fulfilled in the case of powder samples [23–25], but not for macroscopic single crystals and other well-defined samples. In the 1980s, adsorption calorimetry on macroscopic Pt(111) single crystals was attempted using a thermistor as sensor, but the results were discouraging [26]. The decisive breakthrough was achieved by Sir D.A. King (Cambridge, UK) in the 1990s with the usage of ultrathin single crystals with a thickness of only 0.2 μm, in combination with a pulsed molecular beam source and an infrared detector (pyrometer) [27–29]. The heat capacity of such a sample is very low, and even the adsorption of a fraction of a monolayer leads to a significant change in temperature on the order of 1 K [30]. The resulting change in intensity of emitted infrared light can be measured by means of an infrared detector outside the ultrahigh-vacuum (UHV) apparatus. Given a careful setup, heats of adsorption of at least 1 μJ/cm^2 can be measured.

For calibration of the calorimeter, a laser beam with known intensity and closely matched temporal and spatial characteristics as the molecular beam is used to deposit a known amount of heat in the sample. For this calibration, the reflectivity of the sample at the wavelength of the laser must be precisely known. Alternatively, a known heat of reaction, such as the multilayer adsorption energy of the adsorbate, may be used to calibrate the system. Although used in Schuster's electrochemical calorimeter (see below) this approach is typically not used for ultrahigh vacuum calorimeters, except to confirm the laser-based calibration.

To determine the heat of adsorption per molecule (or per mol), the number of adsorbed molecules in each pulse must be known. This number is determined by separate measurements of flux and sticking probabilities. The flux is measured with a stagnation gauge. The sticking probability is measured by a mass spectrometer, detecting the reflected molecules (King-Wells techniques [31], see Fig. 2.4). Before and after each experiment, an inert gold flag is placed in front of the sample, providing the mass spectrometer signal corresponding to 100 % reflection. Because the sticking probability is always measured by comparing with 100 % reflection, the relative uncertainty becomes larger the lower the sticking probability becomes, and unless extreme care is taken, it is generally not possible to measure reliable adsorption energies for sticking probabilities below 10 %. From the measured amounts of heat and the corresponding numbers of molecules, the molar heat of adsorption can be calculated for each pulse. In the limit of very small pulses ($\Delta\Theta \rightarrow 0$), this is a differential heat of adsorption (see Fig. 2.2).

The magnitude of the infrared signal depends strongly on the absolute sample temperature, because the radiant power, ΔP_{rad}, follows the Stefan-Boltzmann law: $\Delta P_{rad} \propto T^3 \Delta T$. This technique will, therefore, have a lower sensitivity at lower sample temperatures and a higher sensitivity at higher sample temperatures. However, cooling or heating of the sample via the support ring is impossible since lateral heat transfer is extremely ineffective. Thus, the sample temperature is dominated by radiative thermalization with the environment. To date, no attempts have been made to measure at sample temperatures above or below room temperature, e.g., by means of a cryoshroud.
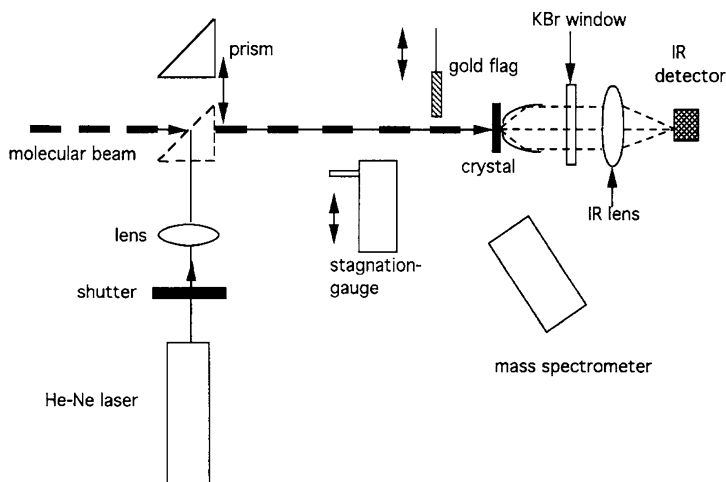
Fig. 2.4 Single-crystal calorimeter by D.A. King. The adsorption-induced temperature change of the thin single-crystal sample (0.2 μm) is measured with an IR detector outside the UHV apparatus (*right*). For dosing, a pulsed molecular beam is used (*left*). Further components: pulsed laser beam for calibration (*left*), stagnation gauge for flux measurements (*center*), and mass spectrometer and gold flag for measurements of the sticking probability after King and Wells [31] (reproduced from Refs. [27–29] with permission from Elsevier B.V., © 1996)
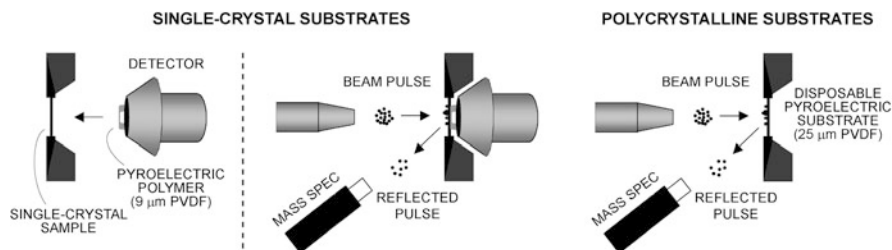

Fig. 2.5 An illustration of the Campbell calorimeter. *Left*: The setup for single-crystalline samples. A thin pyroelectric polymer ribbon is mounted in an arch and pressed gently against the backside of the sample. As a pulse of molecules adsorbs on the single-crystal sample, heat is deposited and is detected as a temperature change in the pyroelectric polymer. Simultaneously, the sticking probability of the molecular pulse is measured by a mass spectrometer, detecting the reflected fraction of the pulse. *Right*: The setup for polymer samples, organic films and other polycrystalline samples, which are deposited as thin films directly on the detector

2.3.3 Single-Crystal Adsorption Calorimeter by C.T. Campbell

The central feature of the single-crystal calorimeter by C.T. Campbell et al. is a pyroelectric detector, which gently contacts the backside of a thin single-crystal sample during the measurement (Fig. 2.5). The material of the detector is a pyro-electric polymer, typically 9 μm thick β-polyvinylidene fluoride (β-PVDF) in the
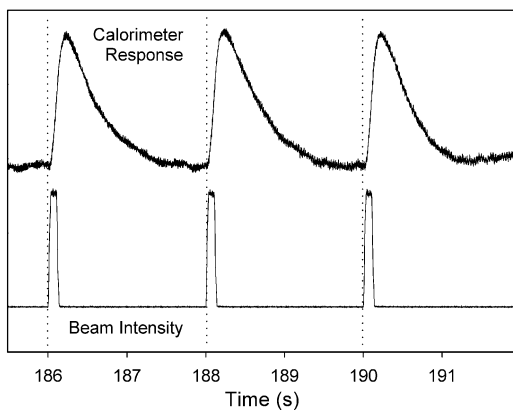
form of a bent ribbon. The direct mechanical contact between sample and detector requires thicker samples than those used in the King calorimeter, typically 1 μm or thicker, but leads to an increased sensitivity, such that temperature changes in the μK range can be detected. The increased sensitivity allows samples as thick as 100 μm to be used [32–35]. This represents a considerable advantage, since 100 μm thick samples may be produced by mechanically thinning down readily available thicker single-crystal samples. The thin 1 and 0.2 μm single-crystal samples are produced as epitaxially grown films on a salt crystal and are therefore only available for certain elements and surface orientations. The smooth and mirror-like surfaces of the 100 μm samples is another advantage, because the calibration of the calorimeter requires the knowledge of the reflectivity of the sample. The reflectivity is difficult to measure accurately on the buckled surfaces of the thin 0.2–1 μm foils.

Because the heat transfer between sample and detector is efficient even at low temperatures, low-temperature measurements are possible and have been carried out with the Campbell design [36]. The upper operating temperature of the Campbell design is around 400 K, where a significant degradation of the detector will start to occur. During sample preparation, which normally includes annealing at high temperatures, the detector is retracted from the sample and does not limit the maximum annealing temperature.

The adsorbate is dosed by means of a periodically pulsed molecular beam. For gases or liquids with vapor pressures above 10 mbar at room temperature, an effusive beam is used. For metals or other solids with low vapor pressures an evaporator is used instead. The pulses have a typical length of 100 ms and a frequency of 0.5 Hz. Each pulse leads to the deposition of heat in the sample and causes a detector signal, which is proportional to the temperature increase and, thus, to the amount of heat (Fig. 2.6). Note that a pyroelectric detector is a current source, for which the current is proportional to the time derivative of the temperature, $I_{pyro} \sim dT/dt$. Calibration is achieved with a laser, as in King's setup.

In the Campbell design the flux of the molecular beam is measured before and after each experiment with a Quartz Crystal Microbalance (QCM) positioned in front of the sample. When used to measure the flux of molecules such as benzene

or cyclohexene, the QCM is cooled with liquid nitrogen to allow multilayers to build up. For adsorbates with negligible vapor pressure at room temperature, such as metals, cooling of the QCM is not necessary. As in King's setup, the sticking probability is measured by a mass spectrometer, detecting the reflected molecules, see Fig. 2.5. For metals and other low vapor pressure compounds the inert flag, used to calibrate the mass spectrometer, is heated to ensure 100 % reflection.

If the molecular beam is produced by a hot source, as for example in the case of metals or compounds with low vapor pressure, then the contribution from the absorbed IR radiation to the calorimeter signal must be measured separately. For this purpose, an IR transmissive window, such as BaF_2 or KBr, is inserted in the beam path, blocking the molecules or atoms in the beam, but allowing the radiation to reach the sample.

The Campbell design has produced several offspring; one such has been constructed by R. Schäfer's group in Darmstadt [38, 39]. Schäfer's design involves a novel pulsed molecular beam, which, instead of the typical continuous beam chopped by a rotating chopper, uses an intrinsic pulsed beam. The pulses are created by a piezoelectric plunger, opening and closing to a gas containing vessel of known volume. After an experiment the gas dose per pulse can be determined by measuring the pressure drop in the gas containing volume and dividing by the number of pulses. The pressure changes are typical in the range of 10^{-4} mbar (at a starting pressure in the range of 1 mbar) and are measured by a capacitance pressure gauge.

2.3.4 Electrochemical Single-Crystal Adsorption Calorimeter by R. Schuster

All the single-crystal calorimeters discussed this far have been ultrahigh vacuum-based calorimeters, where the adsorbate is dosed from the gas phase in an ultrahigh vacuum chamber onto a single-crystal surface. However, in the group of R. Schuster the technique has been adapted to measure heat effects during electrochemical reactions, with conversions of just a few percent of a monolayer [40–43]. Similar to Campbell's design a pyroelectric polymer foil is used as the detector (Fig. 2.7). In Campbell's design the soft contact between the pyroelectric polymer detector and the sample limits the heat transfer into the detector. Schuster solved this problem by evacuating the space between the detector and the sample, allowing the ambient pressure in the electrochemical cell to press the detector and sample together, forming a tight contact. The samples are typically 12 μm thick single or polycrystalline metal foils supported by a 120 μm thick Si sheet. The Si support is used to reduce bending of the sample/detector sandwich, which would cause false signals since the PVDF-based detector is piezoelectric as well as pyroelectric.

An interesting feature of the electrochemical calorimeter is that for electrochemical reactions conducted close to equilibrium the heat effects reflect the entropy changes at the interface. Whereas the ultrahigh vacuum-based calorimeters measure reaction energies, Schuster's electrochemical calorimeter measures reaction
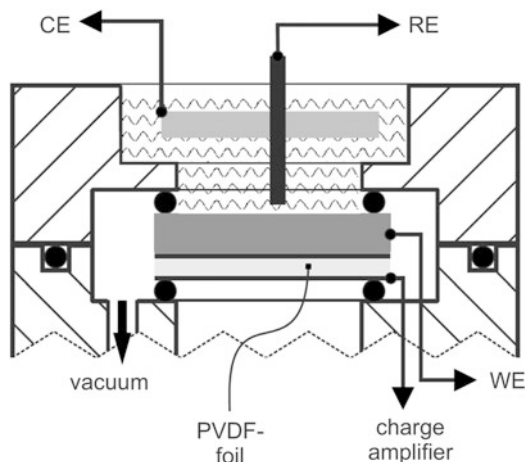
Fig. 2.7 Electrochemical cell of the calorimeter by R. Schuster et al. [40–42]. The sample (working electrode, WE) is located directly above the detector (PVDF foil). To increase the mechanical stability of thin samples, a 120 μm thick Si sheet may be inserted between the sample and the detector. A good mechanical contact between sample and detector is achieved by evacuating the volume between sample and detector. CE: counter electrode; RE: reference electrode (reproduced from Ref. [40] with permission from the American Institute of Physics, © 2010)

entropies. Schuster's calorimeter is also much smaller and simpler than the large ultrahigh vacuum calorimeters, but the interpretation of the measurements is far more complex than those for ultrahigh vacuum-based calorimeters. The sensitivity of the method is in the range of 1 μJ/cm^2 and thus, despite the presence of the liquid phase, only 1–2 orders of magnitude below that of UHV calorimeters [41]. However, because of heat loss into the liquid, Schuster's calorimeter operates with much faster pulses than the ultrahigh vacuum calorimeters, typically in the range of 10 ms, see Fig. 2.8. Calibration of the calorimeter is achieved by using an electron transfer reaction, such as the $[Fe(CN)_6]^{4-}/[Fe(CN)_6]^{3-}$ redox system, depositing a known amount of heat [40]. Schuster's technique has been used to measure the deposition and dissolution of Ag and Cu as well as phase transitions in organic monolayers on electrode surfaces [40–43].

2.4 Applications of the Technique

### 2.4.1 Surface Phase Transitions—CO Adsorption on Pt

Surface phase transitions or reconstructions are frequently occurring phenomena and are often induced or lifted by adsorbates on the surface. An example is CO and ethylene adsorption on Pt(100). Unreconstructed Pt(100)-(1 × 1) can be prepared at 300 K, but the unreconstructed phase is metastable, and upon heating to 500 K

Fig. 2.8 The deposition (**a**) and dissolution (**b**) of Ag onto a 300 ML thick silver film on Au. At $t = 0$ the potential was stepped to 5 mV negative (**a**) or positive (**b**), and after 10 ms the cell current was forced to 0. During deposition the sample temperature increases with time, which can be attributed to the reduction in entropy of the electrode-solution interface by the removal of Ag ions from solution (reproduced from Ref. [40] with permission from the American Institute of Physics, © 2010)
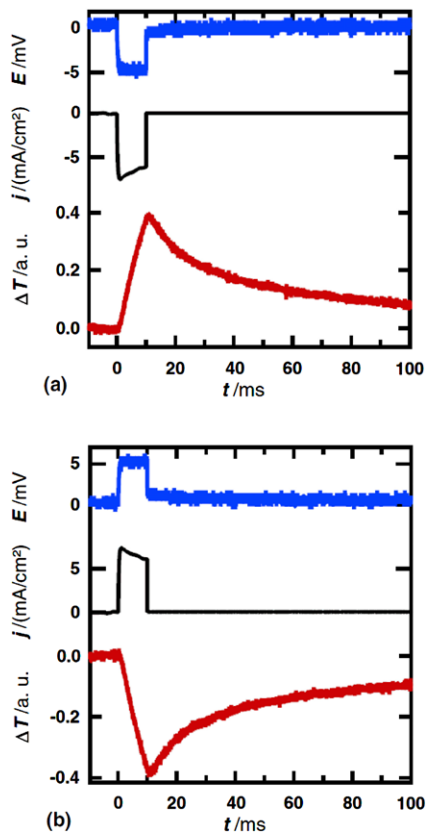
the surface will reconstruct to Pt(100)-hex, adopting a hexagonal arrangement in the first layer. Upon adsorption of CO or ethylene at 300 K the reconstruction is lifted, and the final state of the surface is identical to the final state when CO or ethylene is adsorbed on the unreconstructed Pt(100)-(1 × 1) surface. The reconstruction energy can therefore be measured directly with single-crystal adsorption calorimetry as the difference in the integrated adsorption energies, yielding an energy difference between Pt(111)-hex and Pt(100)-(1 × 1) of 20–25 kJ/mol [44].

Single-crystal adsorption calorimetry was also used to investigate the energetics of the Pt(311)-(1 × 2) surface reconstruction [45]. This reconstruction was—albeit with some discrepancy in their findings—observed by Blakely and Somorjai [46] and Gaussmann and Kruse [47, 48] and more recently studied by means of DFT by Orita and Inada [49]. Using a combination of calorimetry and low-energy electron diffraction (LEED), it was possible to confirm the existence of the reconstruction and to show that the presence of small amounts of CO or carbon are sufficient to lift the (1 × 2) reconstruction [45]. The heats of adsorption for CO on Pt(311)-(1 × 2) and Pt(110)-(1 × 2) are shown in Fig. 2.9. For CO adsorption on Pt(311) four distinct adsorption regions can be observed, each corresponding to different adsorption structures.
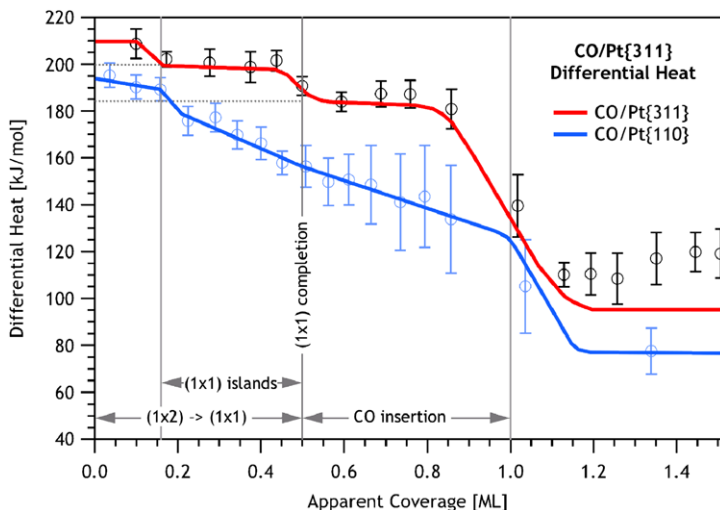
Fig. 2.9 Coverage-dependent differential heats of adsorption for CO on Pt(311) (*red lines*) and Pt(110) (*blue lines*) adsorbed at 300 K. Open circles are averaged experimental data points (error bars represent one standard deviation from averaging across several experiments), and the solid lines represent guides to the eye through these points (CO/Pt(110) data adapted from Refs. [50, 51] with permission from the American Chemical Society, © 1996 and 1998)

2.4.2 Reaction Intermediates—Cyclohexene Adsorption on Pt(111)

Platinum is an excellent hydrogenation/dehydrogenation catalyst and the adsorption of hydrocarbons on platinum has therefore received much attention in the literature. However, because many hydrocarbons readily dehydrogenate on platinum before any desorption occurs, desorption-based techniques, such as temperature programmed desorption, are very limited in their ability to study these systems. Let us consider the hydrogenation of benzene to cyclohexane. It is one of the first steps in the production of nylon, but may also be seen as a model reaction for the removal of aromatics in diesel. From a more fundamental point of view, this is a system with a wide range of interesting possible reaction intermediates that are not accessible using desorption-based techniques. An example is the adsorption of cyclohexene, a possible reaction intermediate, on Pt(111), see Fig. 2.10. At 100 K, cyclohexene adsorbs intact, but as the surface is heated, sequential dehydrogenation will occur, eventually resulting in adsorbed graphite.

Unlike temperature programmed desorption, single-crystal calorimetry does not rely on desorption and can therefore directly measure the heat of adsorption and reaction of the wealth of species formed as hydrocarbons are adsorbed on platinum. However, to control the species formed upon adsorption, it is necessary to control the temperature, at which the measurement is carried out. With the Campbell design this is possible, and Fig. 2.11 shows the experimental differential heat of adsorption of cyclohexene on Pt(111) at 100 K as an example. In the range of the first
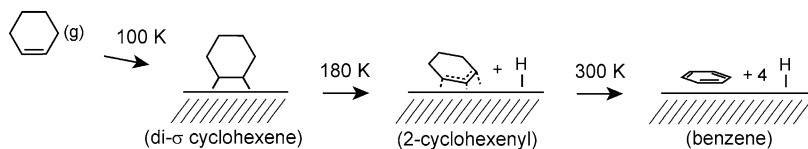
Fig. 2.10 The temperature dependent, sequential dehydrogenation of cyclohexene on Pt(111) [36]. At 100 K, cyclohexene adsorbs intact forming a di-bonded cyclohexene species. Above 180 K, cyclohexene looses an allylic hydrogen, forming a conjugated 2-cyclohexenyl intermediate. Above 300 K, three more hydrogen atoms are abstracted and adsorbed benzene and hydrogen are formed. Above room temperature, the adsorbed hydrogen will desorb, and around 400 K benzene will further dehydrogenate, eventually producing graphite at high temperatures. By controlling the adsorption temperature, it is therefore possible, using the same starting molecule, to measure the heat of formation of multiple different intermediates

adsorbed layer ($\Theta < 0.24$ ML) [37], the heat of adsorption decreases with growing coverage, which indicates repulsive interactions between the adsorbed molecules. Based on the shape of the curve, conclusions regarding the strengths of these interactions can be made [52, 53]. Using the heat of adsorption at very low coverages ($\Theta \rightarrow 0$, 130 kJ/mol), the standard enthalpy of formation of adsorbed cyclohexene (-135 kJ/mol) and the dissociation energy of the Pt–C bond (205 kJ/mol) were calculated. Both values are not accessible by any other technique than adsorption calorimetry. After saturation of the first layer ($\Theta > 0.24$ ML), the heat of adsorption has a constant value of 47 kJ/mol. This value represents the heat of condensation of cyclohexene at 100 K, since the molecules adsorb here on molecular layers and the influence of the substrate is negligible. Similar investigations were performed for benzene and naphthalene on Pt(111) [52, 53]. Based on these measurements and values for the other above-mentioned temperature ranges, a complex energy landscape for the hydrogenation of benzene to cyclohexane on Pt(111) can be derived [54]. Such data are of great importance for the quantitative understanding of heterogeneous catalytic reactions.

From the standard deviation between the data points in the multilayer range in Fig. 2.11, it can be concluded that a heat of adsorption of approximately 5 kJ/mol represents the detection limit for the calorimeter used here. This corresponds to a sensitivity limit of approximately 100 nJ/cm^2, if the active sample area is taken into account. The ability of the Campbell design to carry out experiments below room temperature has also been used to measured the heat of formation of adsorbed hydroxyl on Pt(111), by adsorbing water on an oxygen pre-covered Pt(111) surface at 150 K [55, 56].

2.4.3 Metal Adsorption on Polymers—Calcium on Poly(3-Hexylthiophene)

For some systems, desorption-based techniques are inappropriate because the adsorbate will thermally decompose before or simultaneous with desorption. For other

Fig. 2.11 Differential heat of adsorption of cyclohexene on Pt(111) at 100 K (*open circles*) and the integral heat of adsorption (*dotted line* in the range $0 < \Theta < 0.24$ ML), calculated using (2.10) (reproduced from Ref. [36] with permission from the American Chemical Society, © 2008)
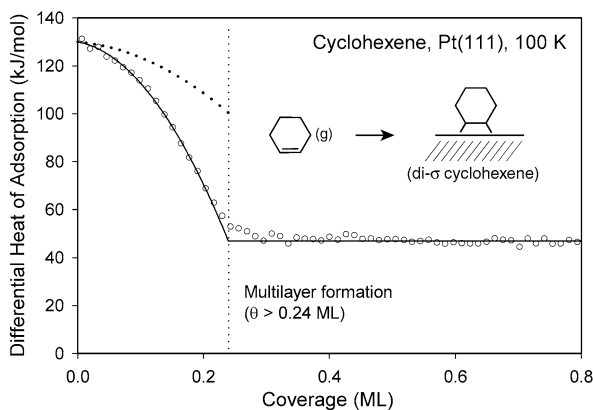

systems, it is the substrate which will decompose. This is the case for metal adsorption on organic substrates [57–60]. Such interfaces occur in organic electronic or opto-electronic devices [61, 62]. An important parameter in this respect is the interface energy, because it determines the stability of the interface and is related to its electronic properties. For example, the charge injection rates at the interface depend on the overlap of wave functions and thus on the character of the interfacial chemical bond [63]. For polycrystalline or amorphous films, the organic film can, as shown in Fig. 2.5, be deposited directly on the detector, for example by vacuum sublimation or spin coating. The benefit of depositing the substrate film directly on the detector is that the sensitivity is increased by more than an order of magnitude.

As an example, we will discuss the adsorption of Ca on the π-conjugated, semiconducting polymer poly(3-hexylthiophene), P3HT, which leads to formation of a complex metal/organic interface. This is also a good example of how single-crystal adsorption calorimetry today is no longer restricted to single-crystal studies, but is used as a general technique for a wide range of planar, low surface area samples. The differential heat of adsorption of Ca on P3HT as a function of coverage is shown in Fig. 2.12. From the initial value is 625 kJ/mol (adsorption on defect sites), the heat of adsorption drops rapidly to 405 kJ/mol, which is still considerably larger than the sublimation enthalpy of Ca, 178 kJ/mol. This indicates a strong metal-polymer interaction or a chemical reaction at the interface. Indeed, parallel spectroscopic investigations show that Ca reacts with the thiophene units of the polymer forming calcium sulfide (CaS). This reaction occurs up to a maximum depth of 3 nm at 300 K. If the deposition is performed at lower temperatures, the reaction depth is smaller [57, 64]. This reaction dominates in the early stages of deposition, while Ca particles and finally a closed Ca film form at higher Ca coverages (> 0.5 ML). For this reason, the heat of adsorption slowly approaches the heat of sublimation of Ca and reaches this value around 5 ML. Above this coverage, all newly adsorbing Ca atoms contribute exclusively to the growth of this Ca layer.

The third competing process, the reflection of impinging Ca atoms, prevails at small coverages (initial sticking probability $S_0 = 0.35$), but becomes less important

Fig. 2.12 Differential heat of adsorption of Ca on poly(3-hexylthiophene) at 300 K. A coverage of 1 ML corresponds to a closed-packed Ca(111) layer ($7.4 \cdot 10^{14}$ atoms/cm^2) (adapted from Ref. [54] with permission from the American Chemical Society, © 2010)
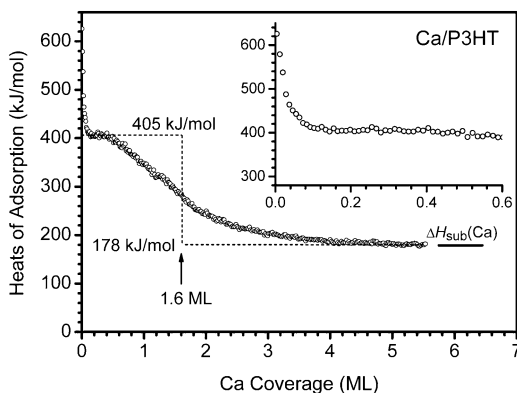
Fig. 2.13 Sticking probability of Ca atoms on poly(3-hexylthiophene) at 300 K, as measured by a modified King-Wells technique [31] (adapted from Ref. [58] with permission from the American Chemical Society, © 2010)
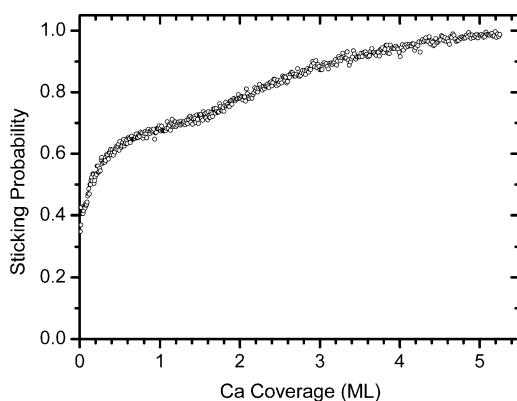

at higher coverages. This is evident from the dependence of the sticking probability on the coverage (Fig. 2.13).

2.4.4 Particle-Size Dependent Adsorption Energies—CO on Pd

Another offspring of the Campbell design is S. Schauermann's and H.-J. Freund's calorimeter in Berlin [65, 66]. It features several technical improvements which potentially reduce systematic errors in the calibration of the calorimeter, for example a system for *in situ* measurements of the reflectivity and an *in situ* photodiode for measuring the power of the calibration laser. Furthermore, it comprises a rotatable table for the precise alignment of sample, photodiode and stagnation gauge in exactly the same position. The construction of this table also ensures improved temperature stability and reduced susceptibility to vibrations.

The Berlin calorimeter has been used to measure the particle-size dependent heats of adsorption on planar model catalysts. For example, the adsorption of CO on Pd nanoparticles on Fe_3O_4 thin films has been studied, see Fig. 2.14. The growth
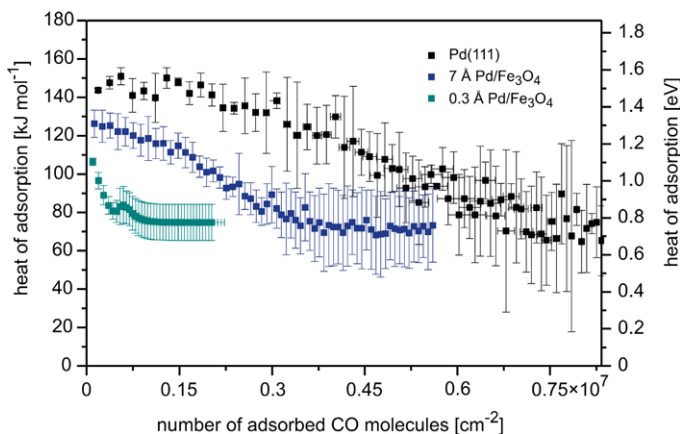
Fig. 2.14 The heat of adsorption of CO on Pd(111) and Pd/Fe$_3$O$_4$/Pt(111) model catalysts. The heat of adsorption is seen to decrease with decreasing particle size (reproduced from Ref. [66] with permission from the American Physical Society, © 2010)

of oxide films on the thin single crystals needed for calorimetry represents a major challenge in these experiments, because the sample temperature must be precisely controlled during the film growth. Since the thin samples must be mounted on a holder with a much larger heat capacity, this is difficult to achieve. During radiative heating, the edges of the thin foils are in contact with the sample holder and will remain relatively colder than the center of the foil, which is far away from the edges. Nevertheless, this challenge has been successfully overcome.

2.5 Future Developments of the Technique

Single-crystal adsorption calorimetry is a very versatile technique and has been used to study a broad range of different low-surface area systems, both single- and polycrystalline. This development is expected to continue, and in the future we may see calorimetric measurements involving adsorption of large organic or bio molecules, intercalation of metals in organic films, or even measurements of the heat of formation of metal-organic or covalent networks on surfaces. Such complex surface reactions often require a precise control of the temperature. It is therefore likely that we will see more measurements above and below room temperature and the development of more apparatus capable of operating under these conditions.

We are also likely to see more sophisticated data treatments. The standard laser calibration used today for ultrahigh-vacuum calorimeters is only valid if the heat of adsorption in the actual calorimetric measurements is deposited instantaneously. However, this is not always the case. The initial adsorption may be followed by a secondary slower reaction, such as decomposition, diffusion into the subsurface range, or desorption. This will cause the shape of the calorimeter response to change,

and the new shape will contain kinetic information about the secondary reaction. As the sensitivities and signal/noise ratios of future calorimeters are expected to increase, it may become possible to deconvolute the calorimeter responses and extract this kinetic information.

Overall, we are likely to see further differentiation, because the technique will be adapted to the systems studied. There will not be one solution equally suitable for all systems. For example, different adsorbates require different molecular beam setups. Thin 1 μm single-crystal foils may be used when high sensitivity is required, e.g., for deconvolution of the calorimeter response, but thicker 100 μm crystals may be preferred for accuracy, since reflectivity measurements are easier on thicker crystals. Accuracy may also be increased by using laser wavelengths at which the samples have lower reflectivities. For example, gold and copper have reflectivities of 96 % and 92 % at 633 nm, respectively, but only 37 % and 50 % at 405 nm [67]. We may also see advanced sample mounts which will provide better temperature control for preparation of oxide thin films and model catalysts.

Radiative contributions to the calorimeter signal will be a challenge for adsorption studies with many catalytically relevant transition metals. As the evaporation temperature required increases, the heat of adsorption becomes a smaller signal on an increasing background of radiated heat. Calorimetry has already been used to measure the growth of Ag on CeO_2 and MgO [68], but attempts to move to metals with even lower vapor pressures requires refining our techniques for measuring the radiation contribution. Radiation may also represent a challenge at lower temperatures if both the evaporant and the sample have high emissivities in the far infrared region. In those cases, simple infrared transmissive windows such as BaF_2 or KBr may not transmit over a wide enough range, and alternative solutions may have to be considered, such as Au or Ag mirrors or rotating velocity filters [69], which are only transmissive for the molecules and completely eliminate the radiative contribution to the calorimeter signal.

Finally, as this technique becomes more wide-spread, we are likely to see more experimental overlaps. If the same system is investigated with more than one calorimeter, experimental accuracy and reliability will improve. Today, the best way to determine the accuracy of a calorimetric measurement is to compare it to known values, such as the heats of adsorption in the multilayer range to tabulated heats of sublimation. This approach is especially feasible for adsorption of metals. However, for many systems, such direct comparisons are not possible.

References

1. H.-J. Freund, Principles of chemisorption, in *Handbook of Heterogeneous Catalysis*, vol. 3, ed. by G. Ertl, H. Knözinger, J. Weitkamp (VCH Wiley, Weinheim, 1997), p. 911
2. M. Boudart, Principles of heterogeneous catalysis, in *Handbook of Heterogeneous Catalysis*, vol. 1, ed. by G. Ertl, H. Knözinger, J. Weitkamp (VCH Wiley, Weinheim, 1997), pp. 1–13
3. D.A. King, Surf. Sci. **47**, 384 (1975)
4. K. Christmann, *Introduction to Surface Physical Chemistry* (Steinkopff, Darmstadt, 1991)
5. T. Fujita, W. Kobayashi, C. Oshima, Surf. Interface Anal. **37**, 120 (2005)

6. G. Comsa, R. David, Surf. Sci. Rep. **5**, 145 (1985)
7. J.K. Roberts, Proc. R. Soc. Lond. A **152**, 445 (1935).
8. J.K. Roberts, Proc. R. Soc. Lond. A **152**, 464 (1935)
9. J.K. Roberts, Proc. R. Soc. Lond. A **152**, 477 (1935)
10. P. Kisliuk, J. Chem. Phys. **31**, 1605 (1959)
11. S. Černý, Surf. Sci. Rep. **26**, 1 (1996)
12. O. Beeck, Rev. Mod. Phys. **17**, 61 (1945)
13. O. Beeck, W.A. Cole, A. Wheeler, Discuss. Faraday Soc. **8**, 314 (1950)
14. G. Wedler, Z. Phys. Chem. **24**, 73 (1960)
15. G. Wedler, Z. Phys. Chem. **27**, 388 (1961)
16. G. Wedler, H. Strothenk, Ber. Bunsenges. Phys. Chem. **70**, 214 (1966).
17. G. Wedler, I. Ganzmann, D. Borgmann, Ber. Bunsenges. Phys. Chem. **97**, 293 (1993)
18. M. Kovář, L. Dvořák, S. Černý, Appl. Surf. Sci. **74**, 51 (1994)
19. J.K. Gimzewski, Ch. Gerber, E. Meyer, R.R. Schlittler, Chem. Phys. Lett. **217**, 589 (1994)
20. J.R. Barnes, R.J. Stephenson, M.E. Welland, Ch. Gerber, J.K. Gimzewski, Nature **372**, 79 (1994)
21. J.R. Barnes, R.J. Stephenson, C.N. Woodburn, S.J. O'Shea, M.E. Welland, T. Rayment, J.K. Gimzewski, Ch. Gerber, Rev. Sci. Instrum. **65**, 3793 (1994)
22. J.M. Antonietti, J. Gong, V. Habibpour, M.A. Rottgen, S. Abbet, C.J. Harding, M. Arenz, U. Heiz, C. Gerber, Rev. Sci. Instrum. **78**, 054101 (2007)
23. B.E. Spiewak, R.D. Cortright, J.A. Dumesic, Thermochemical characterization, in *Handbook of Heterogeneous Catalysis*, vol. 3, ed. by G. Ertl, H. Knözinger, J. Weitkamp (VCH Wiley, Weinheim, 1997), p. 698
24. R. Naumann d'Alnoncourt, M. Bergmann, J. Strunk, E. Löffler, O. Hinrichsen, M. Muhler, Thermochim. Acta **434**, 132 (2005)
25. L. Damjanovic, A. Auroux, Heterogeneous catalysis on solids, in *Handbook of Thermal Analysis and Calorimetry*. Recent Advances, Techniques and Applications, vol. 5, ed. by M.E. Brown, P.K. Gallagher (Elsevier, Amsterdam, 2008), p. 387
26. D.A. Kyser, R.J. Masel, Rev. Sci. Instrum. **58**, 2141 (1987)
27. C.E. Borroni-Bird, N. Al-Sarraf, S. Andersoon, D.A. King, Chem. Phys. Lett. **183**, 516 (1991)
28. A. Stuck, C.E. Wartnaby, Y.Y. Yeo, J.T. Stuckless, N. Al-Sarraf, D.A. King, Surf. Sci. **349**, 229 (1996)
29. W.A. Brown, R. Kose, D.A. King, Chem. Rev. **98**, 797 (1998)
30. R. Kose, New frontiers in single crystal adsorption calorimetry, Dissertation, Downing College, University of Cambridge, 1998
31. D.A. King, M.G. Wells, Proc. R. Soc. Lond. A **339**, 245 (1974)
32. J.T. Stuckless, N.A. Frei, C.T. Campbell, Rev. Sci. Instrum. **69**, 2427 (1998)
33. C.T. Campbell, O. Lytken, Surf. Sci. **603**, 1365 (2009)
34. S.F. Diaz, J.F. Zhu, N. Shamir, C.T. Campbell, Sens. Actuators B **107**, 454 (2005)
35. W. Lew, O. Lytken, J.A. Farmer, M.C. Crowe, C.T. Campbell, Rev. Sci. Instrum. **81**, 024102 (2010)
36. O. Lytken, W. Lew, J.J.W. Harris, E.K. Vestergaard, J.M. Gottfried, C.T. Campbell, J. Am. Chem. Soc. **130**, 10247 (2008)
37. The coverage Θ (with the unit ML) is here defined as the number of adsorbate molecules divided by the number of surface atoms (for Pt(111) 1.505 10^{15} cm^{-2}). A complete first layer of cyclohexene on Pt(111) at 100 K is reached at a coverage of $\Theta = 0.24$ ML
38. A. Schießer, R. Schäfer, Rev. Sci. Instrum. **80**, 086103 (2009)
39. A. Schießer, P. Hörtz, R. Schäfer, Surf. Sci. **604**, 2098 (2010)
40. K.D. Etzel, K.R. Bickel, R. Schuster, Rev. Sci. Instrum. **81**, 034101 (2010)
41. K.D. Etzel, K.R. Bickel, R. Schuster, Chem. Phys. Chem. **11**, 1416 (2010)
42. R. Schuster, R. Rösch, A.E. Timm, Z. Phys. Chem. **221**, 1479 (2007)
43. K.R. Bickel, K.D. Etzel, A.E. Timm, D. Nattland, R. Schuster, in *Hauptversammlung der Deutschen Bunsen-Gesellschaft für Physikalische Chemie*, Bielefeld, 13–15 May 2010
44. Y.Y. Yeo, C.E. Wartnaby, D.A. King, Science **268**, 1731 (1995)

45. R. Kose, D.A. King, Chem. Phys. Lett. **313**, 1–6 (1999)
46. D.W. Blakely, G.A. Somorjai, Surf. Sci. **65**, 419–442 (1977)
47. A. Gaussmann, N. Kruse, Surf. Sci. **266**, 46–50 (1992)
48. A. Gaussmann, N. Kruse, Surf. Sci. **279**, 319–327 (1992)
49. H. Orita, Y. Inada, J. Phys. Chem. B **109**, 22469–22475 (2005)
50. C.E. Wartnaby, A. Stuck, Y.Y. Yeo, D.A. King, J. Phys. Chem. **100**, 12483–12488 (1996)
51. W.A. Brown, R. Kose, D.A. King, Chem. Rev. **98**, 797–832 (1998)
52. H. Ihm, H.M. Ajo, J.M. Gottfried, P. Bera, C.T. Campbell, J. Phys. Chem. B **108**, 14627 (2004)
53. J.M. Gottfried, E.K. Vestergaard, P. Bera, C.T. Campbell, J. Phys. Chem. B **110**, 17539 (2006)
54. O. Lytken, W. Lew, C.T. Campbell, Chem. Soc. Rev. **37**, 2172 (2008)
55. W. Lew, M.C. Crowe, E. Karp, O. Lytken, J.A. Farmer, L. Arnadóttir, C. Schoenbaum, C.T. Campbell, J. Phys. Chem. C **115**, 11586 (2011)
56. W. Lew, M.C. Crowe, C.T. Campbell, J. Carrasco, A. Michaelides, J. Phys. Chem. C **115**, 23008 (2011)
57. F. Bebensee, J. Zhu, J.H. Baricuatro, J.A. Farmer, Y. Bai, H.-P. Steinrück, C.T. Campbell, J.M. Gottfried, Langmuir **26**, 9632–9639 (2010)
58. J. Zhu, F. Bebensee, W. Hieringer, W. Zhao, J.H. Baricuatro, J.A. Farmer, Y. Bai, H.-P. Steinrück, J.M. Gottfried, C.T. Campbell, J. Am. Chem. Soc. **131**, 13498 (2009)
59. R. Murdey, J.T. Stuckless, J. Am. Chem. Soc. **125**, 3995 (2003)
60. J. Zhu, P. Goetsch, N. Ruzycki, C.T. Campbell, J. Am. Chem. Soc. **129**, 6432 (2007)
61. R.H. Friend, Pure Appl. Chem. **73**, 425 (2001)
62. F. Faupel, V. Zaporojtchenko, T. Strunskus, J. Erichsen, K. Dolgner, A. Thran, M. Kiene, Fundamental aspects of polymer metallization, in *Metallization of Polymers 2*, ed. by E. Sacher (Kluwer Academic, New York, 2002)
63. C.H. Schwalb, S. Sachs, M. Marks, A. Schöll, F. Reinert, E. Umbach, U. Höfer, Phys. Rev. Lett. **101**, 146801 (2008)
64. F. Bebensee, M. Schmid, H.-P. Steinrück, C.T. Campbell, J.M. Gottfried, J. Am. Chem. Soc. **132**, 12163 (2010)
65. J.-H. Fischer-Wolfarth, J. Hartmann, J.A. Farmer, J.M. Flores-Camacho, C.T. Campbell, S. Schauermann, H.-J. Freund, Rev. Sci. Instrum. **82**, 024102 (2011)
66. J.-H. Fischer-Wolfarth, J.A. Farmer, J.M. Flores-Camacho, A. Genest, I.V. Yudanov, N. Rösch, C.T. Campbell, S. Schauermann, H.-J. Freund, Phys. Rev. B **81**, 241416 (2010)
67. D.R. Lide, *CRC Handbook of Chemistry and Physics*, 88th edn. (Internet Version 2008) (CRC Press/Taylor and Francis, Boca Raton)
68. J.A. Farmer, C.T. Campbell, Science **329**, 933 (2010)
69. R. Murdey, S.J.S. Liang, J.T. Stuckless, Rev. Sci. Instrum. **76**, 023911 (2005)